Assessment of Cancer Recurrence in Residual Tumors after Fractionated Radiotherapy: A Comparison of Fluorodeoxyglucose, L-Methionine and Thymidine

Michael J. Reinhardt, Kazuo Kubota, Susumu Yamada, Ren Iwata and Hiroshi Yaegashi

Department of Nuclear Medicine and Radiology and Department of Pathology, Institute of Development, Aging and Cancer and Cyclotron and Radioisotope Center, Tohoku University, Sendai, Japan

This study evaluates the midterm follow-up of tumor and normal tissue uptake of deoxyglucose, thymidine and methionine after fractionated radiotherapy to assess cancer recurrence in residual tumors. **Methods:** AH109A tumor-burdened rats were treated with one to eight doses of 5Gy ^{60}Co radiation. Tissue distribution study with ^{18}F-FDG, ^{3}H-thymidine and ^{14}C-methionine, double-tracer autoradiography with ^{18}F-FDG and ^{14}C-methionine, and single-tracer autoradiography with ^{14}C-labeled deoxyglucose, thymidine and methionine were performed 6 days after the end of therapy. **Results:** Dose response study shows a significant decrease of tumor uptake of all tracers after two and more doses, even in the case of later recurrence. Whereas ^{3}H-Thd and ^{14}C-Met tumor uptake was similar to that of normal muscle, ^{18}F-FDG tumor uptake remains higher than that of muscle, even in the case of complete tumor cure. The irradiated muscle shows a higher ^{18}F-FDG uptake than the nonirradiated muscle. Autoradiography after eight doses (100% tumor cure) reveals elevated ^{14}C-DG tumor uptake to be ascribable to nonmalignant cellular elements, in particular to a macrophage layer at the rim of necrotic areas. Autoradiography after four and six doses (33% and 57% tumor cure) shows the highest methionine and thymidine uptake in viable cancer cells, whereas deoxyglucose uptake did not differ between viable cancer cells and macrophages. **Conclusion:** To detect and differentiate viable cancer cells in a residual tumor mass after radiotherapy, PET using ^{11}C-methionine or ^{11}C-thymidine may have some advantages over ^{18}F-FDG, especially if the residual tumor includes larger areas of necrosis.

Key Words: fluorine-18-FDG; carbon-11-methionine; carbon-11-thymidine; fractionated radiotherapy

J Nucl Med 1997; 38:280-287

PET using 2-deoxy-2-^{18}F-fluoro-D-glucose (^{18}F-FDG) and L-methyl-^{11}C-methionine (^{11}C-Met) is well established in the diagnosis and follow-up of cancer (*1–7*). However, the decrease of ^{18}F-FDG tumor uptake after therapy may not necessarily indicate a good prognosis (*2,4,7*), and even a high tumor uptake of ^{18}F-FDG after therapy may not always be consistent with the diagnosis of tumor recurrence (*3,5,8,9*). In a nonirradiated experimental tumor, about 25% of the total tumor uptake of ^{18}F-FDG was derived from nonmalignant cellular elements within the tumor (*10*). Carbon-14-methionine as a substitute for ^{11}C-Met uptake was not significantly influenced by changes in intratumoral components due to its lower accumulation in nonmalignant cellular elements (*11*). The different accumulation of PET tracers may become clinically relevant, in particular after radiotherapy, because inflammation, granulation, fibrosis and necrosis appear in the residual tumor (*12–15*). These changes may not be limited to the tumor itself but may affect the peritumoral normal tissue in the field of radiation as well.

Tumor uptake of ^{14}C-Met and 6-^{3}H-thymidine (^{3}H-Thd) in rat AH109A hepatoma decreased more rapidly than that of ^{18}F-FDG after a 20-Gy single-dose irradiation, despite uptake changes of all three tracers preceding the spread of necrosis and tumor shrinkage (*16*). It remains to be studied whether the initial decrease of tumor uptake can predict the final outcome or whether the tracer uptake by residual tumor mass in the midterm follow-up after fractionated radiotherapy can differentiate recurrence from fibrosis and scar.

It was recently shown that the ^{18}F-FDG uptake of normal tissue does not change significantly after radiotherapy (*17*). Contrary to this, a persistent and significant increase of ^{18}F-FDG uptake in the chest wall of patients treated with external radiation for bronchogenic carcinoma has been observed by others (*18*). Whether methionine and thymidine show similar or different accumulation than deoxyglucose in normal tissue due to irradiation has not been investigated.

This study was designed to elucidate the midterm follow-up of tumor and normal tissue uptake of FDG, L-methionine and thymidine after different radiation doses using a rat AH109A tumor model.

MATERIALS AND METHODS

Animals, Tumors and Irradiation

The experimental protocol for this study, involving animals maintained in the animal laboratory of the Institute of Development, Aging and Cancer, was fully accredited by the Laboratory Animal Care Committee of the Tohoku University.

Five-week-old male Donryu rats were injected subcutaneously on their left thighs with a 0.1-ml suspension containing 7×10^6 cells of syngeneic ascitic hepatoma AH109A. Cobalt-60 irradiation was started 8 days later. The rats were anesthetized with 5 mg sodium pentobarbital intraperitoneally, then fixed with adhesive tape to place the tumor-bearing thigh in the field of irradiation (*19*). The tumors were exposed to single or multiple doses of 5 Gy at a dose rate of 1.03 Gy/min (at 65 cm SSD and 1-cm depth) with a copper aluminum filter. Irradiation was repeated 1, 3, 5 and 7 times with a 24-hr dose interval between two dose fractions.

Tumor Growth Study

Solid tumors were measured using a Vernier caliper every day until the death of each rat. The product of the three principal diameters of tumor was designated as tumor volume (*20*). Six rats per group were used for single-, two- and four-dose irradiation and

Received Dec. 27, 1995; revision accepted July 8, 1996.

For correspondence contact: Michael J. Reinhardt, MD, Department of Nuclear Medicine, Albert-Ludwigs-University Freiburg, Hugstetter Str. 55, D-79106 Freiburg i. Br., Germany.

For reprints contact: Kazuo Kubota, MD, Department of Nuclear Medicine and Radiology, IDAC Tohoku University, Sendai 980, 4-1 Seiryomachi Aoba-Ku, Japan.

seven rats each were used for the six- and eight-dose experiment. To rule out different tracer uptakes due to the procedure of irradiation with repeated anesthesia, a nonirradiated and a sham-irradiated control group were used. Each control group consisted of 12 rats.

Irradiation started when tumor volume was approximately 3500 mm^3 (about 15 mm in diameter). Growth delay was expressed as the time after irradiation for the tumor to grow to double the size it was at the beginning of irradiation. Growth delay of the irradiated tumors was compared to that of the control tumors.

Triple-Tracer Tissue Distribution Study

The tissue distribution study was performed on Day 6 after radiotherapy with single or multiple doses of 5 Gy and nonirradiated controls. A total of 38 tumor-bearing rats, with five to eight rats per group, were used. After 12 hr of fasting, a mixture of three tracers [2.5 MBq ^{18}F-FDG (radiochemical purity > 99%), 185 kBq 6-^{3}H-thymidine (specific activity 851 GBq/mmole, radiochemical purity 99.2%, Amersham Int., UK) and 185 kBq L-methyl-^{14}C-methionine (specific activity 2.04 GBq/mmole, radiochemical purity 99.9%, Amersham Int., UK)] in 0.25 ml of saline was injected through a lateral tail vein. One hour later, the rats were anesthetized and killed. Tissue samples were quickly excised and weighed, followed by ^{18}F measurement by an automated gamma-scintillation counter. Three days later, when ^{18}F had decayed, tissue samples were prepared for liquid scintillation counting of ^{3}H and ^{14}C. Each sample was digested and bleached with 0.5 ml perchloric acid and hydrogen peroxide (1:3) in a heater at 75°C for 2 hr. The samples were mixed with 10 ml of scintillation cocktail and left at room temperature overnight (*16*). Tissue radioactivity was expressed as a differential uptake ratio (DUR) (*19*):

$$\text{DUR} = \frac{\text{tissue counts (cpm)/tissue weight (g)}}{\text{injected dose counts (cpm)/body weight (g)}}.$$

Autoradiography

Seven rats were prepared for autoradiography (ARG) 6 days after four and six doses of 5 Gy ^{60}Co. After fasting overnight, 750 kBq of either 2 deoxy-D-[1-^{14}C]-glucose (specific activity 2.18 GBq/mmole, radiochemical purity > 98%, Amersham Intl., UK), [2-^{14}C] thymidine (specific activity 1.92 GBq/mmole, radiochemical purity 98.1%, Amersham Intl., UK) and ^{14}C-Met were injected through a lateral tail vein, and the rats were killed 1 hr later by an overdose of chloroform. The tumors were quickly dissected, embedded in O.C.T. compound (Miles Inc., Elkhart, IN) and deep frozen on a block of dry ice. Five-μm-thick sections were cut off on a cryostat at −26°C and directly contacted with ARG film (MARG ^{3}H-type, Konica, Japan). After developing the film, sections on the slides were stained with hematoxyline and eosine.

Two rats were prepared for double-tracer ARG 6 days after eight doses of 5-Gy ^{60}Co irradiation. For this, a mixture of 185 MBq ^{18}F-FDG and 750 kBq ^{14}C-Met in 0.5 ml saline was injected. The further procedure was the same as for single-tracer ARG. ARG film exposure was 2–4 hr for ^{18}F and 7–10 days for ^{14}C image.

Semiquantitative evaluation of autoradiograms was done by measuring optical density in the ROIs with a precision densitometer (Sakura PDA 25, Tokyo, Japan) (*21*). To rule out depictable differences in grain size and numbers due to the physical nature of ^{18}F, ^{3}H and ^{14}C, only ^{14}C-labeled tracers were used for quantitation.

Statistics

Analysis of mean DUR and optical density values was done using Student's t-test. A Bonferroni correction was applied for multiple comparisons.

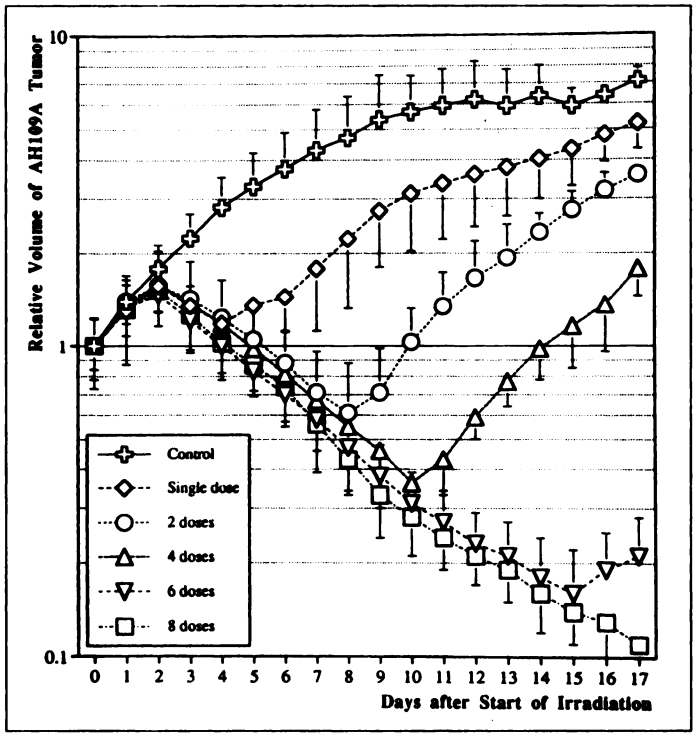

FIGURE 1. AH109A tumor response to different dose fractions. Tumor volume changes are plotted on a logarithmic scale against the time on a linear scale. The relative tumor volume of each group at the beginning of irradiation (Day 0) is designated as 1.

RESULTS

The pattern of response of AH109A tumor growth to different doses of 5-Gy ^{60}Co-irradiation is shown in Figure 1. No significant difference in tumor growth was observed between nonirradiated and sham-irradiated controls. Therefore, only one control group is displayed in the figure. Tumor doubling time was 2.6 days, measured from the beginning of irradiation. Growth delay was 4.9 ± 1.3 days after a single dose, 10.6 ± 1.5 days after two doses and 15 ± 1.2 days after four doses. All differences were significant ($p < 0.001$). Growth delay could not be given for the six- and eight-dose experiments. In the six-dose group, two rats showed a tumor regrowth after therapy but died of distant metastasis before tumor volume reached the size it was at the beginning of radiation. No tumor regrowth was observed in the eight-dose group and the tumor disappeared completely 4–6 wk after radiotherapy. Two rats of the four-dose group and four rats of the six-dose group were cured of their tumors (not shown in the figure). Tumor cure was achieved in 100% after eight doses, in 57% after six doses and in 33% after four doses.

Fluorine-18-FDG (left), ^{3}H-Thd (middle) and ^{14}C-Met (right) uptake of different tissue samples 6 days after radiotherapy with single or multiple fractions of 5 Gy each and of nonirradiated controls is shown in Figure 2. The tumor uptake of all tracers declined rapidly after a single dose ($p < 0.05$ for ^{18}F-FDG, $p < 0.01$ for ^{3}H-Thd and $p < 0.001$ for ^{14}C-Met) but slowly after more than two doses (not significant for all tracers). Muscle from the lower leg, which was in the field of irradiation, shows a significantly higher ^{18}F-FDG uptake than the corresponding nonirradiated muscle from the contralateral thigh after two and more fractions ($p < 0.01$). The tumor uptake of ^{18}F-FDG remained higher than that of irradiated muscle ($p < 0.01$ for single-, two-, six- and eight-dose experiments, not significant for four-dose experiments). Contrary to ^{18}F-FDG, the tumor uptake of ^{3}H-Thd and ^{14}C-Met declined to the level of muscle

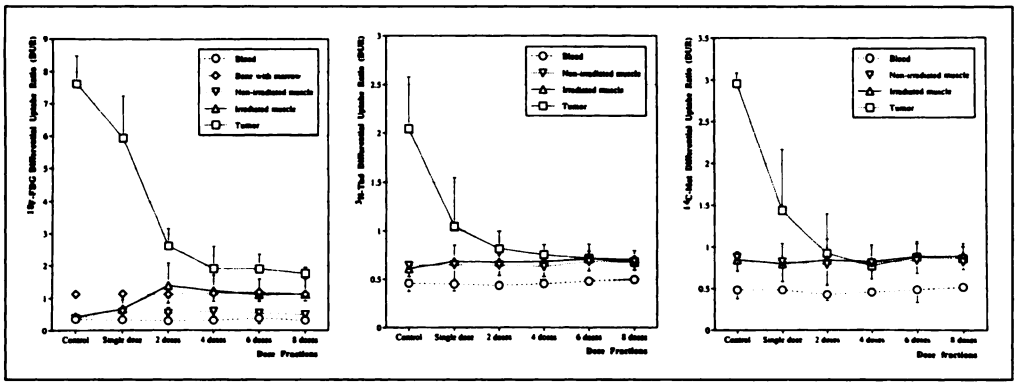

FIGURE 2. The differential uptake ratio (DUR) as a function of dose fractions. The left graph shows the ^{18}F-FDG uptake of tumor and normal tissues, the middle and the right graph show the corresponding values of ^{3}H-Thd and ^{14}C-Met, respectively. For methodological reasons, the DUR of bone and bone marrow could only be determined with ^{18}F-FDG.

with no difference between the irradiated and nonirradiated muscle.

To figure out why tumor uptake of deoxyglucose but not of methionine was higher than that of muscle even in the case of 100% tumor cure, double-tracer ARG with ^{18}F-FDG and ^{14}C-Met was performed after eight doses. Figure 3A shows the ^{18}F-FDG image, Figure 3B the ^{14}C-Met image and Figure 3C the corresponding histologic section. Fluorine-18-FDG is the highest on the rim of central necrosis and on a few spotty dense areas within the tumor. Carbon-14-Met uptake on those areas is not increased. Figure 3D shows a layer of activated macrophages (with clear cytoplasm) between necrosis on the left and degenerating cancer cells on the right to cause the increased ^{18}F-FDG uptake. The spotty dense areas on the ^{18}F-FDG image consist of degenerating cancer cells with significant infiltration of macrophages and fibroblasts (not shown).

Single-tracer ARG with ^{14}C-labeled tracers was performed to assess differentiation of recurrence in a residual tumor before the appearance of regrowth. Figure 4A shows a ^{14}C-Thd ARG of a tumor after six doses. Except for four small areas of increased ^{14}C-Thd uptake, the tumor uptake is homogeneously low. Figure 4B shows the corresponding histologic sample, Figure 4C shows details of the rim of necrosis (arrowhead) and Figure 4D shows one area of increased uptake (arrow). The

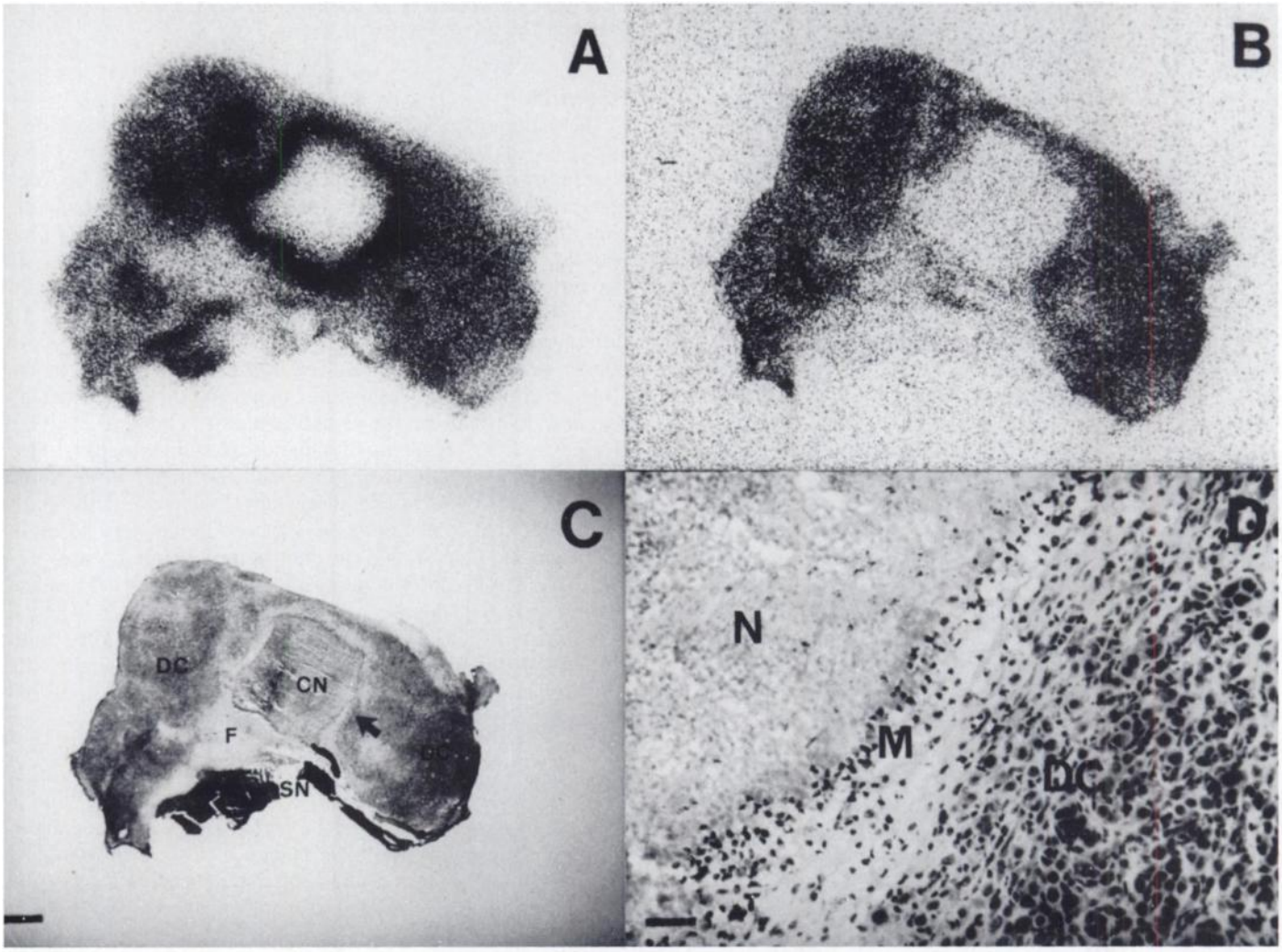

FIGURE 3. Autoradiographs with (A) ^{18}F-FDG and (B) ^{14}C-Met of the (C) same histologic tumor section. Central necrosis (CN), surface necrosis (SN), fibrosis (F) and degenerating cancer cells (DC) with macrophage and fibroblast infiltration can be identified. (D) A 200-fold magnification of the rim of central necrosis (arrow). Necrosis (N), macrophage layer (M) and degenerating cancer cells (DC) can be differentiated. Scale bar is 1 mm for A, B and C and 50 μm for D.

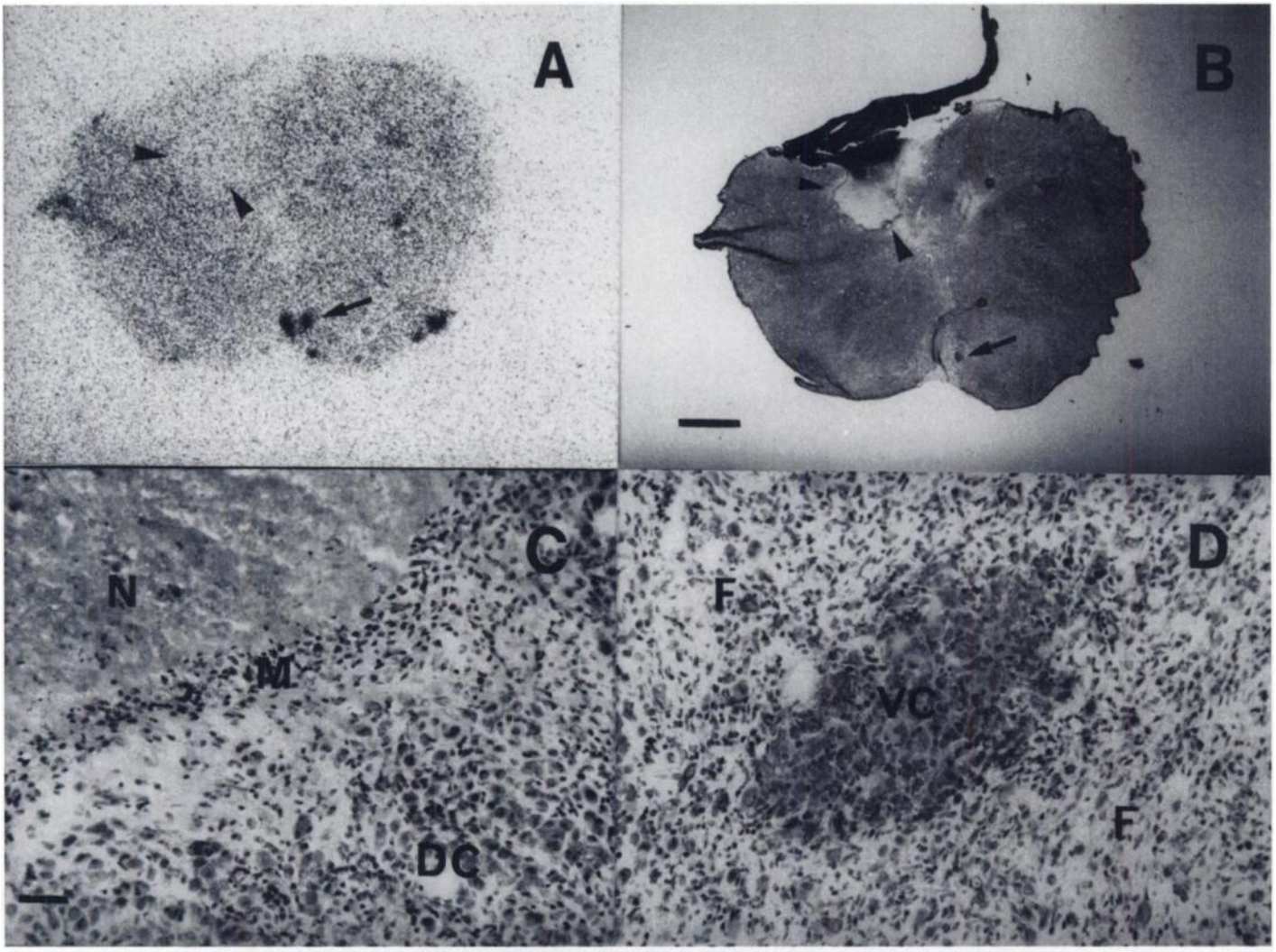

FIGURE 4. (A) ARG with ^{14}C-Thd and (B) corresponding histology of a continuously shrinking tumor. Note some spotty dense areas in the inferior part of the tumor (arrow). (C) Details of the rim of necrosis (arrowheads). (D) A 200-fold magnification of a hot spot (arrow) consisting of viable cancer cells (VC). Necrosis (N), macrophage layer (M), fibrosis (F), viable cancer cells (VC) and degenerating cancer cells (DC) can be differentiated. Scale bar is 1 mm for A and B and 50 μm for C and D.

macrophage layer on the rim of necrosis has almost the same low uptake as areas of degenerating cancer cells with fibroblast and macrophage infiltration. The hot spot consists of an islet of viable cancer cells.

Figure 5A shows the ^{14}C-Met ARG of a tumor after four doses and Figure 5B shows the corresponding histologic section. Methionine uptake is the highest in the periphery of the tumor. The remaining tumor shows a much lower uptake, but inhomogeneity of accumulation pattern was somewhat more distinct than that of thymidine. Figure 5C shows a small necrotic area on the right (arrowheads), having the lowest uptake in the tumor. Carbon-14-Met uptake in the surrounding macrophage layer is not increased. Figure 5D shows details of the tumor periphery, consisting of a solid mass of viable cancer cells (arrow).

Figure 6A shows a ^{14}C-DG ARG of a tumor after four doses, and Figure 6B shows the corresponding histologic section. A central fibrotic area is surrounded by numerous foci of increased deoxyglucose uptake. Figure 6C (white arrow) and 6D (black arrow) show histologic details of two such areas. Note that ^{14}C-DG accumulation of an area consisting of degenerating cancer cells with macrophage and fibroblast infiltration (Fig. 6C) is almost the same as in another area, where cancer cells have started again to form the typical lobular structure of hepatoma and to regrow (Fig. 6D).

Semiquantitative evaluation confirmed visually interpreted intratumoral accumulation pattern of the three tracers (Table 1). Residual tumors after four and six doses that currently did not regrow before Day 6 after radiotherapy were used for this comparison. Compared to degenerating cancer cells, the macrophage uptake of ^{14}C-DG is higher ($p < 0.001$), but the same in the ^{14}C-Thd image and lower in the ^{14}C-Met ARG ($p < 0.01$). Uptake of ^{14}C-Thd and ^{14}C-Met on viable cancer cells is significantly higher than on the macrophage layer at the rim of necrosis ($p < 0.001$), whereas ^{14}C-DG shows no difference. Furthermore, ^{14}C-DG uptake of muscle after irradiation is significantly higher than that of nonirradiated muscle ($p < 0.001$), whereas ^{14}C-Thd and ^{14}C-Met uptake are almost the same.

DISCUSSION

The present study uses a fractionated dose regimen to evaluate the midterm effect of radiotherapy on tumor and normal tissue uptake of deoxyglucose, thymidine and methionine. Fractionation spares normal tissue because of repair of sublethal damage between dose fractions and increases damage to the tumor because of reoxygenation and reassortment of cells into radiosensitive phases of the cycle (*22*). These basic terms of fractionation are confirmed for the rapidly growing AH109A rat tumor when compared to previous single-dose experiments

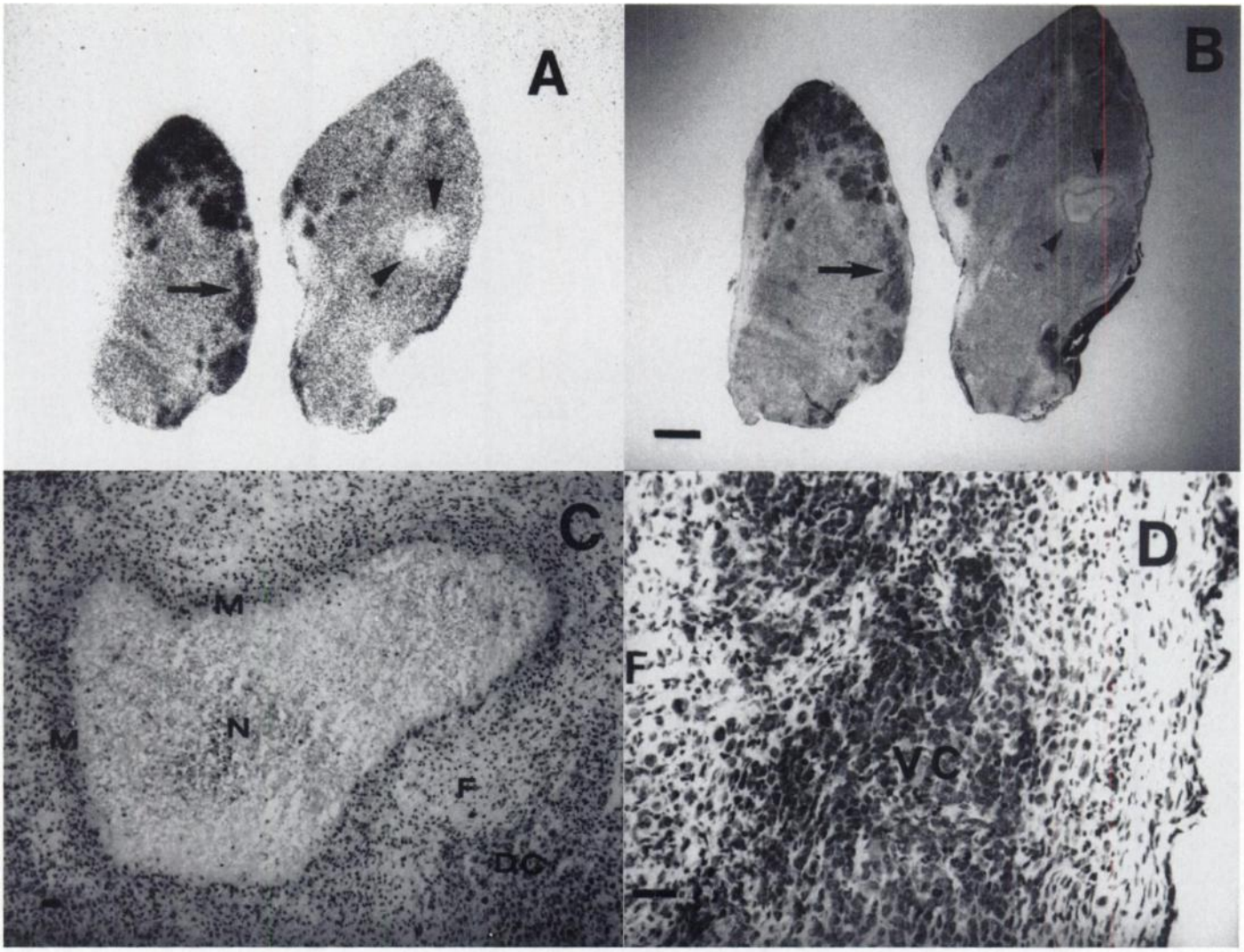

FIGURE 5. (A) ARG with ^{14}C-Met and (B) corresponding histology of a tumor 6 days after four doses. (C) A small necrotic area (arrowheads). (D) Details of an area with increased methionine uptake (arrow); it consists of viable cancer cells. Necrosis (N), macrophage layer (M), fibrosis (F), viable cancer cells (VC) and degenerating cancer cells (DC) can be differentiated. Scale bar is 1 mm for A and B and 50 μm for C and D.

(*16,19*). Growth delay of AH109A after a 10-Gy ^{60}Co radiation is significantly longer when total dose is split into two equal fractions of 5-Gy compared to a single dose (*16*): 10.6 ± 1.5 days compared with 8 ± 1.2 days ($p < 0.01$). The relative tumor volume 10 days after a 20-Gy single dose was 48 ± 10% of that before irradiation (*19*), but 36 ± 9% ($p < 0.05$) when the dose applied is divided into four fractions of 5 Gy each with a 24-hr dose interval. Complete tumor cure could be achieved in 33% after four doses, in 57% after six doses and in 100% after eight doses of 5 Gy ^{60}Co radiation. Therefore, the eight-dose group represents a residual tumor mass without any viable cancer cells, whereas the four- and six-dose groups represent a residual tumor that may regrow. The single- and two-dose groups may be representative for early recurrence.

Multiple-dose fractions require multiple courses of anesthesia given to the rats, which may accelerate tumor growth by suppression of immune response (*23*) or by increasing the radiobiological hypoxic fraction (*24*). However, eightfold administration of 5 mg pentobarbital intraperitoneally in the sham-irradiated control group did not produce a statistically significant difference in the growth of AH109A hepatoma, which is similar to the findings in 9L gliosarcoma-burdened rats (*25*).

This study shows a radiation-induced increase in deoxyglucose uptake of muscle tissue in the field of radiation. Thymidine and methionine uptake on irradiated and nonirradiated muscle remains almost equal. There are few clinical reports depicting an increased ^{18}F-FDG uptake in normal tissue after radiation. Fluorine-18-FDG uptake of the sacral bone was increased in two patients after radiotherapy for rectal cancer without evidence for osseous alteration (*8*). Six months after therapy, ^{18}F-FDG uptake of the chest wall of patients with bronchogenic carcinoma was still found to be 40% higher than before treatment (*18*). On the other hand, overlapping of ^{18}F-FDG uptake in distinguishing between fibrosis and persistent or recurrent cancer after radiation for bronchogenic cancer was relatively small (*26*).

The pathophysiological mechanism underlying the increase of ^{18}F-FDG uptake of irradiated muscle is unknown. Radiation will induce some time- and dose-dependent injuries to normal tissue. Significant damage to the capillary endothelial cells and the vascular basal lamina with subsequent fibrosis has been reported (*13*). An increase of the functional vascular volume was followed by elevated extravasation rate of plasma proteins (*15*). In the mid 1980s, Kairento et al. used PET and ^{15}C oxygen and ^{15}O inhalation technique in rabbits to study regional blood flow and oxygen utilization in muscle (*27*). Regional blood flow increased 95% in the skeletal muscle after three doses of 6-Gy radiation delivered on consecutive days. The regional oxygen extraction fraction increased only 45% in muscle for at least one

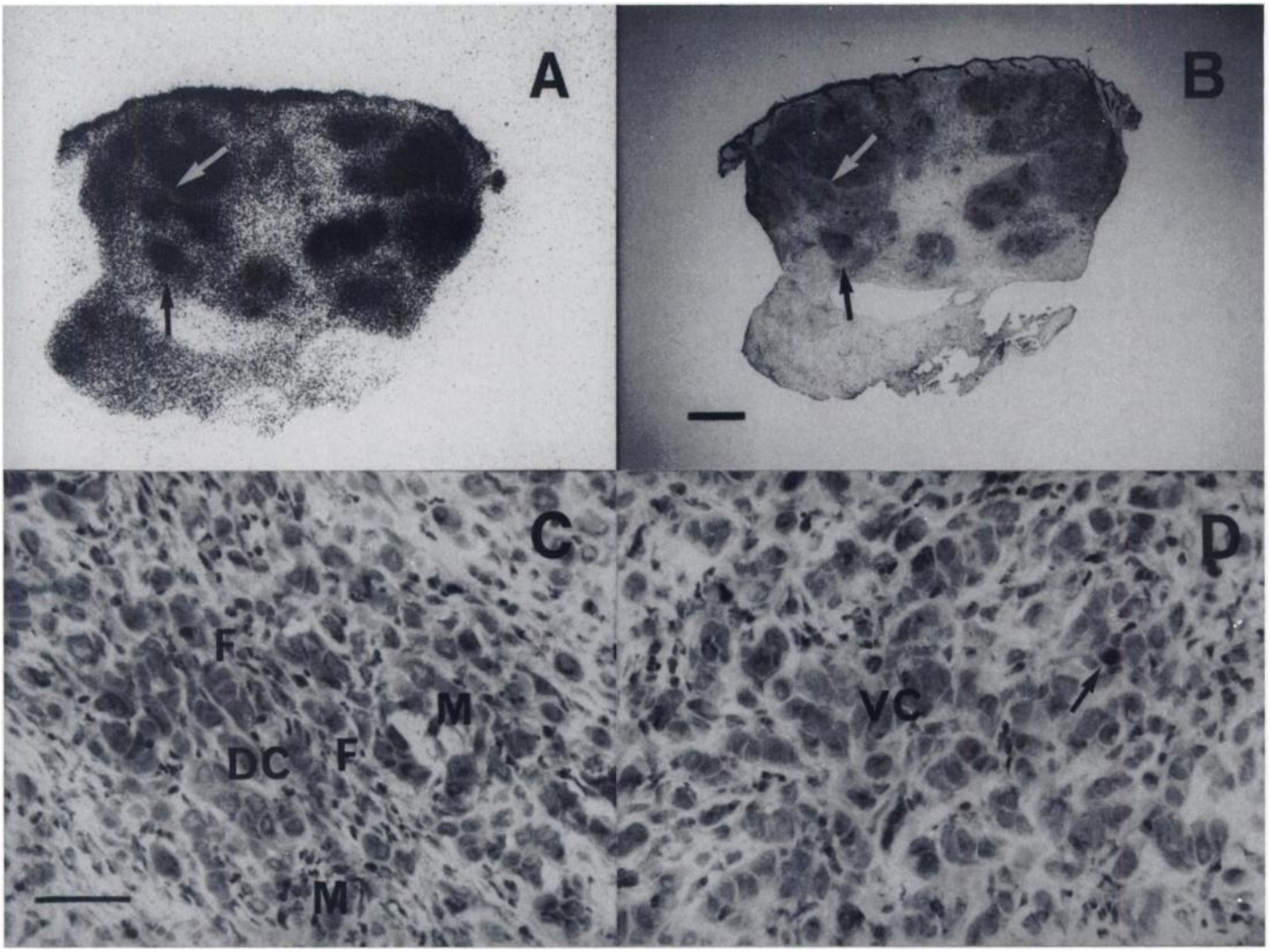

FIGURE 6. (A) ARG with ^{14}C-DG and (B) corresponding histology of a tumor 6 days after four doses. A central fibrotic area is surrounded by some areas of high DG uptake. (C) Some of these areas (white arrow) consist of degenerated cancer cells with massively infiltrating fibroblasts and macrophages and (D) others, as marked with a black arrow, show a beginning regrowth. (D) A mitosis is marked (arrow). Macrophage layer (M), fibrosis (F), viable cancer cells (VC) and degenerating cancer cells (DC) can be differentiated. Scale bar is 1 mm for A and B and 50 μm for C and D.

week (*27*). This difference may be interpreted as hypoxia due to irradiation. In the skeletal muscle, hypoxia induces an adaptive response of increasing cellular glucose uptake through elevated expression of GLUT 1 glucose transporter in an attempt to maintain supply of glucose for utilization by nonoxidative pathways (*28–31*). While muscle uptake of DG increases due to hypoxia, the uptake of amino acids does not change during a hypoxic state (*29*). Exposure to free radicals, as produced by ^{60}Co radiation, may induce an inactivation of the key enzyme of oxidative phosphorylation, the mitochondrial F_0F_1 ATP synthase (*32*). Anaerobic glycolysis, as source of energy, may be increased due to this process (*33*). Because anaerobic glycolysis is less effective than aerobic glycolysis, the glucose transport may increase consecutively. However, enzyme activity and

TABLE 1
Optical Density of Different Tissue Components of AH109A Tumor in Carbon-14-Labeled Autoradiograms with Deoxyglucose, Thymidine and Methionine after Fractionated Radiotherapy (Background-Corrected)

Tissue	Optical density			Ratio relative to muscle		
	^{14}C-DG	^{14}C-Thd	^{14}C-Met	DG	Thd	Met
Viable cancer cells	1.08 ± 0.11	1.02 ± 0.06	1.12 ± 0.06	2.57	2.43	2.54
Degenerating cancer cells*	0.71 ± 0.18	0.44 ± 0.04	0.59 ± 0.05	1.69	1.05	1.34
Macrophage layer	1.06 ± 0.15	0.42 ± 0.03	0.53 ± 0.04	2.52	1.0	1.2
Fibrotic tissue	0.48 ± 0.06	0.40 ± 0.03	0.38 ± 0.05	1.14	0.95	0.86
Necrotic tissue	0.32 ± 0.02	0.37 ± 0.03	0.34 ± 0.02	0.76	0.88	0.77
Irradiated muscle	0.50 ± 0.03	0.41 ± 0.03	0.44 ± 0.04	1.2	0.98	1.0
Nonirradiated muscle	0.42 ± 0.05	0.42 ± 0.03	0.44 ± 0.04	—	—	—

Each value is the mean ± s.d. of 12 measurements of three rats each.
*Includes fibroblasts and few macrophages.

oxygenation of muscle tissue after radiation could not be evaluated in this experiment.

Despite muscle uptake of ^{18}F-FDG increased due to radiotherapy, ^{18}F-FDG uptake of the residual tumor mass was always higher than that of irradiated muscle. Previous experiments had shown that the initial decline of FDG uptake in a tumor after radiation is somewhat slower than that of methionine or thymidine (*16*). Tumor FDG uptake in vivo showed a linear correlation to the percentage of viable tissue after radiotherapy (*34*). In this study, residual tumor mass after eight doses consisted exclusively of nonmalignant cells. Double-tracer ARG revealed elevated FDG uptake of residual tumor mass to be ascribable to macrophages on the rim of necrosis and, to a lesser extent, by fibroblast and macrophage infiltration in areas of degenerating cancer cells.

Despite the magnitude of ^{18}F-FDG tumor uptake changes after radiation is larger than that of methionine and thymidine, tumor uptake of all investigated tracers could not differentiate later recurrence on Day 6 after radiotherapy (Fig. 2). At this time, assessment of recurrence could be done only by the intratumoral accumulation pattern of methionine or thymidine. The uptake of both tracers is more than two times higher in viable cancer cells than in all other cellular elements of the residual tumors (Table 1). Although DG uptake of viable cancer cells is significantly higher than that of areas of degenerating cancer cells with fibroblast and macrophage infiltration, it might be difficult to differentiate viable cancer cells, because DG uptake in the macrophage layer around necrosis is equal to that in viable cancer cells. Enhanced glycolysis, which is characteristic for malignancy, is an activation signal for macrophages as well (*35*), which may have a two to four times higher glucose uptake than viable cancer cells.

In pretreatment studies with FM3A tumors of C3H mice, it has been shown that up to 29% of tumor uptake may be attributed to noncancer cells (*10*). There is a distinct variability on total DG uptake of macrophages: the more aggressive the tumor growth, the higher the total DG uptake of macrophages (*11*). Untreated MH134 and FM3A mouse tumors show a higher ^{18}F-FDG uptake on tumor-associated macrophages than on viable cancer cells, whereas ^{14}C-Met and ^{3}H-Thd uptake was highest on viable cancer cells (*11,36*). Necrobiotic or degenerated cancer cells, which exist as well within the untreated tumor, had almost the same ^{14}C-Met but a higher ^{18}F-FDG uptake than macrophages (*11*). Six days after fractionated radiotherapy of AH109A tumor, these proportions are almost the same for ^{14}C-Met and ^{14}C-Thd uptake. The uptake of ^{18}F-FDG and ^{14}C-DG after radiation is somewhat different: the uptake of viable cancer cells and macrophages is equal but higher than that of necrobiotic or degenerating cancer cells (Table 1). All other cellular components of the residual tumor showed a significantly lower uptake. Relevant FDG-uptake by nonmalignant cellular elements of the tumor may be welcome for pretreatment evaluation because it will increase detectability of smaller tumors and metastases. However, if PET is performed after treatment to differentiate later recurrence in a residual tumor mass, tracer accumulation in noncancer cells is undesirable. It might be difficult to differentiate between cancer recurrence and nonmalignant cellular components that form to a significant degree during the healing process of the tumor for a longer time period after radiotherapy using ^{18}F-FDG. On the other hand, there is no difficulty in assessing cancer recurrence when there is an area of increased ^{11}C-Met or ^{11}C-Thd uptake in a residual tumor mass. Whether these findings on a rat hepatoma can be transferred to the variety of human tumors with different localizations, different growth rates and different biologic hypoxic fractions remain to be studied.

CONCLUSION

The present study has shown in the AH109A tumor that: (a) methionine and thymidine, but not deoxyglucose, enable differentiation of remaining or recurrent viable cancer cells and nonmalignant cellular elements in a residual tumor in the midterm follow-up after radiotherapy; (b) as long as the tumor does not regrow after radiotherapy, the total uptake of deoxyglucose, methionine and thymidine in the residual tumor mass is similarly low, independent of the number of dose fractions and later recurrence; and (c) muscle uptake of deoxyglucose, but not of methionine and thymidine, increases temporarily after irradiation.

ACKNOWLEDGMENTS

We thank Mr. Y. Sugawara for the preparation of histologic samples, R. Kubota, PhD, and Dr. Y. Abe for advice, and Prof. H. Fukuda and Prof. T. Ido and the staff of the Cyclotron and Radioisotope Center, Tohoku University, Sendai, Japan, for their cooperation, Mr. G. Anders and co-workers for photography, and Dr. E. Moser, Chief of the Department of Nuclear Medicine, Albert-Ludwigs-University, Freiburg, Germany, for his continued support. This work was supported by grants-in-aid 06454320 and 06670899 from the Ministry of Education, Science and Culture, Japan, by the Japanese-German Radiological Affiliation and by a fellowship of the Dr. Mildred Scheel Stiftung für Krebshilfe, Germany.

REFERENCES

1. Fujiwara T, Matsuzawa T, Kubota K, et al. Relationship between histologic type of primary lung cancer and carbon-11-L-methionine uptake with positron emission tomography. *J Nucl Med* 1989;30:33–37.
2. Greven KM, Williams DW, Keyes JW, et al. Positron emission tomography of patients with head and neck carcinoma before and after high-dose irradiation. *Cancer* 1994;74:1355–1359.
3. Haberkorn U, Strauss LG, Dimitrakopoulu A, et al. PET studies of fluoro-deoxyglucose metabolism in patients with recurrent colorectal tumors receiving radiotherapy. *J Nucl Med* 1991;32:1485–1490.
4. Ichiya Y, Kubawara Y, Otsuka M, et al. Assessment of response to cancer therapy using fluorine-18-fluorodeoxyglucose and positron emission tomography. *J Nucl Med* 1991;32:1655–1660.
5. Inoue T, Kim EE, Komaki R, et al. Detecting recurrent or residual lung cancer with FDG-PET. *J Nucl Med* 1995;36:788–793.
6. Leskinen-Kallio S, Nagren K, Lehikoinen P, Ruotsalainen U, Teraes M, Joensuu H. Carbon-11-methionine and PET is an effective method to image head and neck cancer. *J Nucl Med* 1992;33:691–695.
7. Minn H, Paul R, Ahonen A. Evaluation of treatment response to radiotherapy in head and neck cancer with fluorine-18-fluorodeoxyglucose. *J Nucl Med* 1988;29:1521–1525.
8. Engenhart R, Kimmig BN, Strauss LG, et al. Therapy monitoring of presacral recurrences after high-dose irradiation: value of PET, CT, CEA and pain score. *Strahlenther Onkol* 1992;168:203–212.
9. Kim EE, Garcia JR, Wong FCL, et al. Differentiation of thoracic tumors from post-treatment changes using PET with F-18 FDG and C-11 methionine [Abstract]. *J Nucl Med* 1994;35:76P.
10. Kubota R, Kubota K, Yamada S, et al. Intratumoral distribution of fluorine-18-fluorodeoxyglucose in vivo: high accumulation in macrophages and granulation tissues studied by microautoradiography. *J Nucl Med* 1992;33:1972–1980.
11. Kubota R, Kubota K, Yamada S, et al. Methionine uptake by tumor tissue: a microautoradiographic comparison with FDG. *J Nucl Med* 1995;36:484–492.
12. Gragoudas ES, Egan KM, Saornil MA, Walsh SM, Albert DM, Seddon JM. The time course after irradiation changes in proton beam treated uveal melanomas. *Ophthalmology* 1993;100:1555–1559.
13. Kobayashi M. The irradiation effects on the cytoskeletons of C3H/He mouse mammary tumor cells and vascular basement membrane in relation to vascular invasion: a model of intraoperative radiotherapy. *Tohoku J Exp Med* 1988;154:71–89.
14. Van Limbergen E, Rijnders A, van der Schueren E, Lerut T, Christiaens R. Cosmetic evaluation of breast conserving treatment for mammary cancer. A quantitative analysis of the influence of radiation dose, fractionation schedules and surgical treatment techniques on cosmetic results. *Radiother Oncol* 1989;16:253–267.
15. Ullrich RL, Casarett GW. Interrelationship between the early inflammatory response and subsequent fibrosis after radiation exposure. *Radiation Research* 1977;72:107–121.
16. Kubota K, Ishiwata K, Kubota R, et al. Tracer feasibility for monitoring tumor radiotherapy: a quadruple tracer study with fluorine-18-fluorodeoxyglucose or fluo-

rine-18-fluorodeoxyuridine, L-[methyl-^{14}C]methionine, [6-^{3}H]thymidine and gallium-67. *J Nucl Med* 1991;32:2118–2123.
17. Rege SD, Chaiken L, Hoh CK, et al. Change induced by radiation therapy in FDG uptake in normal and malignant structures of the head and neck: quantitation with PET. *Radiology* 1993;189:807–812.
18. Lowe VJ, Herbert ME, Hawk TC, Ansher MS, Coleman RE. Chest wall FDG accumulation in serial FDG-PET images in patients being treated for bronchogenic carcinoma with radiation [Abstract]. *J Nucl Med* 1994;35:76P.
19. Kubota K, Matsuzawa T, Takahasi T, et al. Rapid and sensitive response of carbon-11-L-methionine tumor uptake to irradiation. *J Nucl Med* 1989;30:2012–2016.
20. Kubota K, Kubota R, Matsuzawa T. Dose-responsive growth inhibition by glucocorticoid and its receptors in mouse teratocarcinoma OTT6050 in vivo. *Cancer Res* 1983;43:787–793.
21. Kubota K, Ishiwata K, Yamada S, et al. Dose-responsive effect of radiotherapy on the tumor uptake of L-[methyl-^{11}C]methionine; feasibility for monitoring recurrence of tumor. *Nucl Med Biol* 1991;19:27–32.
22. Hall EJ. Time, dose and fractionation in radiotherapy. In: Hall EJ, ed. *Radiobiology for the radiologist*, 4th ed. Philadelphia, PA: Lippincott; 1994:211–229.
23. Lovett EJ, Alderman J, Munster E, Lundy J. Suppressive effects of thiopental and halothane on specific arms of the immune response. *J Surg Oncol* 1980;15:327–334.
24. Steen RG, Wilson DA, Bowser C, Wehrle JP, Glickson JD, Rajan SS. ^{31}P NMR spectroscopic and near infrared spectrophotometric studies of effects of anesthetics on in vivo RIF-1 tumors. *NMR Biomed* 1989;2:87–92.
25. Kimler BF, Liu C, Evans RG, Morantz RA. Effect of pentobarbital on normal brain protection and on the response of 9L rat brain tumor to radiation therapy. *J Neurosurg* 1993;79:577–583.
26. Patz EF, Lowe VJ, Hoffman JM, Paine SS, Harris LK, Goodman PC. Persistent or recurrent bronchogenic carcinoma: detection with PET and 2-[F-18]-2-deoxy-D-glucose. *Radiology* 1994;191:379–382.
27. Kairento AL, Brownell GL, Elmaleh DR, Swartz MR. Comparative measurement of regional blood flow, oxygen and glucose utilization in soft tissue tumor of rabbit with positron imaging. *Br J Radiology* 1985;58:637–643.
28. Cartee GD, Donan AG, Ramlal T, Klip A, Holloszy JO. Stimulation of glucose transport in skeletal muscle by hypoxia. *J Appl Physiol* 1991;70:1593–1600.
29. Bashan N, Burdett E, Hundel HS, Klip A. Regulation of glucose transportand GLUT 1 glucose transporter expression by 3% O2 in muscle cells in culture. *Am J Physiol* 1992;262:682–690.
30. Shetty M, Loeb JN, Ismail-Beigi F. Enhancement of glucose transport in response to inhibition of oxidative metabolism: pre- and posttranslational mechanisms. *Am J Physiol* 1992;262:527–532.
31. Bashan N, Burdett E, Guma A, Sargeant R, Tumiati L, Liu Z, Klip A. Mechanisms of adaptation of glucose transporters to changes in the oxidative chain of muscle and fat cells. *Am J Physiol* 1993;264:430–440.
32. Guerrieri F, Capozza G, Fratello A, Zanotti F, Papa S. Functional and molecular changes in F_0F_1 ATP-synthase of cardiac muscle during aging. *Cardioscience* 1993;4:93–98.
33. Lakatta EG, Yin FC. Myocardial aging: functional alterations and related cellular mechanisms. *Am J Physiol* 1982;242:H927–H941.
34. Kubota K, Kubota R, Yamada S. FDG accumulation in tumor tissue. *J Nucl Med* 1993;34:419–421.
35. Bustos R, Sobrino F. Stimulation of glycolysis as an activation signal in rat peritoneal macrophages. *Biochem J* 1992;282:299–303.
36. Kubota R, Kubota K, Yamada S, Tada M, Ido T, Tamahashi N. Active and passive mechanisms of [fluorine-18] fluorodeoxyglucose uptake by proliferating and prenecrotic cancer cells in vivo: a microautoradiographic study. *J Nucl Med* 1994;35:1067–1075.

Monitoring Gene Therapy with Herpes Simplex Virus Thymidine Kinase in Hepatoma Cells: Uptake of Specific Substrates

Uwe Haberkorn, Annette Altmann, Iris Morr, Karl-Werner Knopf, Christine Germann, Roland Haeckel, Franz Oberdorfer and Gerhard van Kaick

Department of Oncological Diagnostics and Therapy, German Cancer Research Center, Heidelberg, FRG

This study investigates the application of PET with specific substrates for the assesment of enzyme activity after transfer of the herpes simplex virus thymidine kinase (HSV-tk) gene. **Methods:** After transfection of a rat hepatoma cell line with a retroviral vector containing the HSV-tk gene, different clones were established by G418 selection. Uptake measurements were performed up to 48 hr in a TK-expressing cell line and in a control cell line using thymidine (TdR; measured under therapy conditions), fluorodeoxycytidine (FdCyt) and ganciclovir (GCV). Additionally, bystander experiments and inhibition/competition studies were done. **Results:** In TK-expressing cells GCV treatment caused an increased (up to 250%) TdR uptake in the acid-soluble fraction and a decrease to 5.5% in the acid-insoluble fraction. The FdCyt uptake was higher in the TK-expressing cells than in controls with a maximum after 4 hr (12-fold and 3-fold higher in the acid-insoluble and acid-soluble fraction). GCV accumulated up to 180-fold more in the acid-insoluble and 26-fold more in the acid-soluble fraction. GCV uptake occurred mainly by the nucleoside transport systems. Bystander experiments revealed a relation between growth inhibition or GCV uptake and the amount of TK-expressing cells. GCV uptake and growth inhibition were correlated with r = 0.96. **Conclusion:** Assessment of GCV accumulation may serve as an indicator of the enzyme activity and of therapy outcome. TdR may be useful to measure therapy effects on DNA synthesis, whereas the potential of FdCyt has to be investigated in further studies.

Key Words: gene therapy; HSV thymidine kinase; ganciclovir; PET

J Nucl Med 1997; 38:287–294

Received Feb. 12, 1996; revision accepted Jun. 15, 1996.

For correspondence or reprints contact: Uwe Haberkorn, MD, Dept. of Oncological Diagnostics and Therapy, German Cancer Research Center, Im Neuenheimer Feld 280, FRG-Heidelberg 69120, Germany.

Gene therapy is one of the most promising approaches in cancer therapy directed to selectively target and destroy tumor cells. Using recombinant vector systems, suicide genes may be introduced in the malignant cells. These genes encode enzymes, which convert nontoxic prodrugs into highly toxic metabolites. Since retroviruses preferentially infect dividing cells, recombinant retroviral vectors are useful tools for the transfer of genes in proliferating tissues as malignant tumors. Tissue specificity may be achieved by modifying the virus envelope (*1*) or the introduction of tissue or even tumor specific regulatory sequences (*2,3*).

Gene therapy with herpes simplex virus thymidine kinase (HSV-tk) has been performed in a variety of tumor models in vitro and in vivo (*4–9*). In contrast to human thymidine kinase, HSV-tk is less specific and phosphorylates nucleoside analogs such as acyclovir and ganciclovir (GCV) to their monophosphate metabolites (*10*). These monophosphates are subsequently phosphorylated by cellular kinases to the di- and triphosphates. After integration of the GCV metabolites into DNA, chain termination occurs, followed by cell death.

Although it has been shown that not all tumor cells have to be infected to obtain a sufficient therapeutic response (*6,8,9*), repeated injections of the recombinant retroviruses may be necessary until a therapeutic level of enzyme activity in the tumor is reached. Therefore, planning and individualization of gene therapy with the HSV-tk suicide system necessitates the assessment of suicide gene expression in the tumor to decide if: repeated gene transductions of the tumor are necessary, and to establish a therapeutic window of maximum gene expression